CFD MODELING OF ELECTROSTATIC FORCES IN GAS-SOLID FLUIDIZED BEDS AND THE ROLE OF PROCESS UPSETS

Ram G. ROKKAM[1], Rodney O. FOX[1] and Michael E. MUHLE[2]

[1] Department of Chemical & Biological Engineering, Iowa State University, Ames, IA, USA
[2] Univation Technologies, Baytown, TX, USA

ABSTRACT

Electrostatic charges in gas-solid fluidized beds are known to influence the bed dynamics, bubble shape and size, particle agglomeration, segregation and entrainment. In practice, accumulation of electrostatic charges in fluidized beds can lead to operational issues. The present work focuses on the modeling of electrostatics in gas-solid fluidized beds. The particles are assumed to carry a prescribed size-dependent charge, and charge generation and dissipation are not included. To consider the effects of bi-polar charging the polarity of the charge carried by fine particles is taken opposite to that of coarse particles. The magnitude of particle charges is approximated to realistic charges reported in the literature. The principal objective is to develop a multi-fluid Euler-Euler model that can describe electrostatic forces on charged particles in gas-solid fluidized beds. The multi-fluid model is solved in a commercial CFD code (Ansys Fluent 6.3) and uses the kinetic theory of granular flow for calculating solids pressure and viscosities. The electric field, generated by the presence of charged particles, is solved for at every time step in the time-dependent simulation. The electrostatic forces, proportional to the gradient of the electric field and the particle charge, lead to charge-dependent segregation of particles. The electrostatic model has been developed and applied to a two-dimensional fluidized bed. Charge-dependent segregation is found to vary with the polarity and magnitude of the charge on the solid phase as a function of the particle size.

NOMENCLATURE

B magnetic field
C collision term
d diameter of solid phase
d_{avg} average size of solid phase
E electric field
f distribution function
$f_{g\alpha}$ gas-solid interaction force
$f_{\beta\alpha}$ solid-solid interaction force
$F_{qs\alpha}$ electrostatic force on α^{th} solid phase
F_p force acting on each particle
g specific gravity
m_p mass of each particle
q_{avg} average charge on solid phase

$q_{s\alpha}$ charge on α^{th} solid phase
$p_{s\alpha}$ pressure in the αth solid phase
p_g pressure in gas phase
$v_{s\alpha}$ velocity of αth solid phase
ε_g volume fraction of gas phase
$\varepsilon_{s\alpha}$ volume fraction of αth solid phase
$\in_0$ permittivity of vacuum
$\in_m$ permittivity of mixture
$\bar{\bar{\tau}}_{s\alpha}$ stress tensor of αth solid phase
φ electric potential

INTRODUCTION

Gas-phase processes use fluidized beds for the production of linear low-density (LLDPE) and high-density polyethylene (HDPE). They are more advantageous than liquid-phase processes as they have low capital investment, low operational cost, no solvent extraction, large heat-removal capacity, as well as the capability to utilize different catalysts and produce a wide range of products. However, there is potential for particle agglomeration and sintering. Agglomeration can be caused by thermal and/or electrostatic effects (Hendrickson, 2006). Electrostatics are known to influence the fluidized-bed dynamics, bubble size and shape, thereby effecting the circulation of solids. Charge generation of polymer particles occurs due to particle-particle and particle-wall contact. This phenomenon of charging is known as *triboelectrification* (Cross, 1987). When the electrostatic charge on the polymer particles exceeds a critical value, the electrostatic forces and temperature effects can cause the temperature of the polymer particles to increase above the melting point of the polymer and this causes the polymer particles to agglomerate. Over a period of time these agglomerates gain weight and drop off and accumulate near the distributor plate. The agglomerates in the extreme case can cause partial plugging of the distributor plate and prevent the gas flow and finally cause defluidization.

The present work focuses on the modeling of particle segregation due to electrostatic-induced hydrodynamics effects. Hendrickson (2006) reviews electrostatic effects in polymerization fluidized-bed reactors and explains the charge distribution, causes of bipolar charging, electrostatic charge generation and dissipation mechanisms, and compares the effect of electrostatic

forces with other forces like drag and gravity on particle entrainment. Baron et al. (1987) studied the effects of electrostatics on fine particle entrainment and observed that entrainment was reduced with a decrease of relative humidity. Briens et al. (1992) conducted experiments with polyethylene particles and showed that the smallest particles are not the most easily elutriated from fluidized beds with size ranging from 69 micron catalyst particles to 400 micron polyethylene particles. They found more entrainment when the bed is neutralized. The reason for the reduced entrainment could be that the small particles are attached to the larger particles or are captured by the formation of layers on the reactor walls. Fang et al. (2008) conducted experiments to study the charge and electric potential in a fluidized bed. They concluded that voltage polarity reverses at the free surface, and that bed-level zones are more prone to particle-wall adhesion and wall sheets. Mehrani et al. (2005) developed an online measurement technique using a Faraday cage cup method to understand the charge generation due to particle-gas contact and, in the range of conditions studied, it was found to have negligible effects due to particle-gas contact. They concluded that the build-up of charge is due to the entrained fines. Mehrani et al. (2007) also performed experiments to study the changes of electrostatic behavior after the addition of fines and their experimental results supported the theory of bipolar charging. The fines carried charge opposite to the larger particles and they also observed particles on the walls of the fluidized bed.

In this work, we develop a computational fluid dynamics (CFD) model for polymerization fluidized-bed reactors that includes the effects of electrostatics on particle dynamics. Gas-solid fluidized beds can be modelled using two approaches, namely Euler-Lagrange and Euler-Euler models. The Euler-Lagrange models (van der Hoef et al, 2008) consider the gas phase as a continuum and Newton's equations are solved for each solid phase at the particle level. The trajectory and motion of each particle is calculated at each time step and this increases the required computational resources so there is a limitation of the number of particles used in large-scale simulations. The Euler-Euler models (Fan & Fox, 2008) treat the gas and solid phases as interpenetrating continua. The solid pressure and viscosity are obtained using the kinetic theory of granular flow and frictional theory. These models can be used to simulate large-scale reactors like pilot-plant or commercial reactors. In this work an Euler-Euler model is used to model a pilot-plant-scale polymerization fluidized-bed reactor.

Mahdi et al. (2002) analyzed gas-solid flow in a vertical riser using a steady-state, time-averaged, one-dimensional model (i.e. gradients in the radial direction). They neglected hydrodynamic segregation and studied radial segregation due to the presence of charge on particles. They assumed a prescribed charge on all particles and observed strong radial segregation in the riser under certain conditions. Shih et al. (1987) used a two-fluid model to study the shapes and sizes of bubbles with and without an electric field and assumed a fixed charge on particles. They did simulations on a two-dimensional bed with a central jet and simulated a flow time of one second. The model did not consider the effect of the presence of solid phase in the electrostatic model. The above two works on electrostatics were for monodisperse cases. In

this work we develop an electrostatic model and couple it with a multi-fluid CFD code for time-dependent, 3-D simulations. In this model we consider polydisperse effects and segregation due to electrostatics and hydrodynamics. Since we have a particle size distribution the model is able to explain the effects of bipolar charging. The electric field is computed at every grid point and time step. Using the quadrature method of moments (QMOM), three solid phases are used to represent the polymer particle size distribution (Fan & Fox, 2008). The volume fractions of each solid phase are obtained from the weights and abscissas found using QMOM (Fan et al, 2007). The charge on each solid phase is assumed to be a function of the particle size and is used as an input to the electrostatic model.

This work is divided into three sections. In the first section a description of the electrostatic model is given. The second section deals with the application of the electrostatic model to a pilot-plant polymerization fluidized-bed reactor. The final section reports our conclusions.

MULTI-FLUID CFD MODEL

The multi-fluid CFD model (Fan & Fox, 2008) solves the mass and momentum balances of the gas and solid phases. The model is based on the assumption of interpenetrating continua. The solid-phase equations are derived using the kinetic theory of granular flow (Gidaspow, 1994), which is developed in analogy with the kinetic theory of dense gases. Particles can transport mass, momentum or energy by kinetic transport or by collision interactions. The transport mechanisms can be modeled using the Boltzmann-Enskog equation:

$$\frac{\partial f}{\partial t} + v \frac{\partial f}{\partial x} + \frac{\partial}{\partial v}\left(f \frac{F_p}{m_p} \right) = C \qquad (1)$$

where $f(v;x,t)$ is the velocity distribution function, v is the particle velocity vector, m_p is the particle mass, F_p is the force acting on each particle, which comprises of gas-solid drag, gravitational and electrostatic forces, and C is the collision term. The collision and external force terms need to be closed. Continuity, momentum, and granular temperature equations for the solid phase can be derived from the Boltzmann-Enskog equation and the derivation can be found in the literature (Gidaspow, 1994). In order to describe particles with different sizes and/or charges, the two-fluid model can be extended into a multi-fluid model. In this work we consider multiple solid phases with different sizes and electrostatic charges. The momentum equation for the αth solid phase is

$$\frac{\partial}{\partial t}\left(\varepsilon_{s\alpha}\rho_{s\alpha}v_{s\alpha} \right) + \nabla.\left(\varepsilon_{s\alpha}\rho_{s\alpha}v_{s\alpha}v_{s\alpha} \right) = -\varepsilon_{s\alpha}\nabla p_g - \nabla p_{s\alpha}$$

$$+\nabla.\overline{\overline{\tau}}_{s\alpha} - f_{g\alpha} + \sum_{\alpha=1}^{N} f_{\beta\alpha} + \varepsilon_{s\alpha}\rho_{s\alpha}g + F_{qs\alpha} \qquad (2)$$

where $\varepsilon_{s\alpha},\rho_{s\alpha},v_{s\alpha}$ are the volume fraction, density and velocity of the αth solid phase respectively, $p_{s\alpha},\overline{\overline{\tau}}_{s\alpha}$ are the pressure and stress tensor of the αth solid phase, p_g is the gas pressure, $f_{g\alpha}$ is the interaction force between

the gas and the αth solid phase, $f_{\beta\alpha}$ is the interaction force between the βth and α^{th} solid phases, and $F_{qs\alpha}$ is the electrostatic force acting on the αth solid phase. The gas-solid interaction term is closed by the Gidaspow drag law and the solid-solid interaction term by the Syamlal model. The objective of this work is to develop an electrostatic model for $F_{qs\alpha}$ and this will be discussed in detail below.

Polymerization kinetics and QMOM

A wide range of phenomena with disparate length and time scales are involved in the production of polyethylene using fluidized-bed reactors. A simple mechanistic scheme (Fan et al, 2007) is used to describe the microscale polymerization kinetics. The fundamental reactions considered are the initiation, propagation and termination of the active sites. A uniformly distributed lumped thermal model is used to represent the mesoscale phenomena and a chemical reaction engineering model solves the mass, energy and species balance for an individual growing particle. The catalyst size distribution is represented by a few nodes using the QMOM and the CRE (chemical reaction engineering) model (Fan et al, 2007) is applied on the nodes and the final polymer size distribution is obtained. The CFD model is now initialized with the polymer PSD (particle size distribution). The results from the CRE and multi-fluid model can be used to describe the macroscale phenomena such as segregation, elutriation in the reactor. This macroscale information is useful in design and scale-up of fluidized-bed polymerization reactors

Electrostatic model

The governing equations describing electromagnetic phenomena can be obtained from the well-known Maxwell equations (Jackson, 1999). The Maxwell equations along with the Lorentz force equation (Jackson, 1999),

$$F = q(E + v \times B) \qquad (3)$$

describe the force acting on a point charge in the presence of electromagnetic fields. In most applications of gas-solid flows the particle-phase velocity is much less than the speed of light and hence the force due to the magnetic field can be neglected. The Lorentz force can then be reduced to $F = qE$. Gauss's law in differential form is

$$\nabla \cdot (\in_m \in_0 E) = \rho \qquad (4)$$

The relative permittivity $(\in_m)$ for a gas-solid mixture can be obtained from the Bruggeman equation (Tortora et al, 2005):

$$\varepsilon_g = \left(\frac{\in_s - \in_m}{\in_s - \in_g}\right)\left(\frac{\in_g}{\in_m}\right)^{\frac{1}{3}} \qquad (5)$$

which calculates the permittivity of the gas-solid mixture if the relative permittivity of pure gas and solid are known. The total electric charge density ρ is given by

$$\rho = \sum_{\alpha=1}^{N} q_{s\alpha}\varepsilon_{s\alpha} \qquad (6)$$

where $q_{s\alpha}$ is the charge on the αth solid phase per unit volume and $\varepsilon_{s\alpha}$ is the volume fraction of the αth solid phase. Substituting the permittivity of the gas-solid mixture and charge density in the electric field equation and using the relation $E = -\nabla\varphi$ we obtain an equation for the electric potential (φ) given the particle charge:

$$\nabla \cdot \left(\varepsilon_g\left(\frac{2.17}{\varepsilon_g} - 1.20\right)\nabla\phi\right) = -\sum_{\alpha=1}^{N} \frac{q_{s\alpha}\varepsilon_{s\alpha}}{\in_0} \qquad (7)$$

This Poisson equation is coupled with the multi-fluid CFD model through the volume fractions of the gas and solid phases, and thus must be solved at every time step in the CFD simulation. In this work, the wall boundary condition for the electric potential is zero (i.e., the walls are assumed to be grounded).The electrostatic force acting on the αth solid phase is

$$F_{qs\alpha} = -q_{s\alpha}\varepsilon_{s\alpha}\nabla\varphi \qquad (8)$$

The static charge $q_{s\alpha}$ as a function of particle size is a required input for the model.

Coupling of electrostatic and multi-fluid models

As described above, the electrostatic model needs to be coupled with the multi-fluid CFD model. The algorithm for the coupling is shown in **Figure 1**.

Step 1: Using QMOM three nodes are used to represent the polymer size distribution. The weights and abscissas yield the diameter and volume fraction of each solid phase.
Step 2: The multi-fluid model is initialized with the volume fraction calculated in step 1. The multiphase equations are solved at every time step and grid point. From the multi-fluid model we obtain the volume fractions of the gas and solid phases.
Step 3: Solve the Poisson equation (Eq. 7) for the electric potential using the volume fractions of the gas and solid phases from step 2 and the user-defined specified charges.
Step 3: Evaluate the electrostatic force (Eq. 8) using the gradient of the electric potential.
Step 4: Add electrostatic force to each of the solid-phase momentum equations and repeat steps 2-4 for the next iteration.

RESULTS

The CFD model is applied to a pilot-plant fluidized-bed reactor. A sketch of a typical pilot-plant polymerization fluidized-bed reactor is shown in **Figure 2.** The reactor consists of three zones, a fluidized-bed zone, a disengagement zone and a dome section. The top of the tapered disengagement zone has a larger diameter (~2-4D) than the fluidized zone (D) so as to reduce the gas velocity
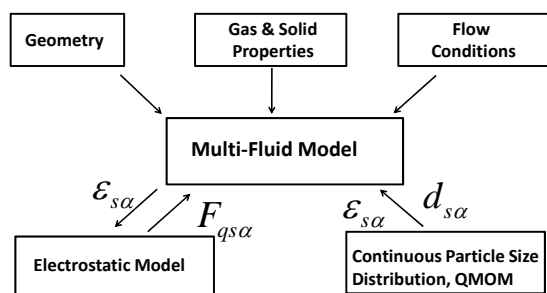
Figure 1: Coupling of electrostatic and multi-fluid CFD model.

to prevent entrainment of polymer particles. Gas along with catalyst particles is injected through the distributor plate. The height of the fluidized-bed zone is ~4-8 D and the disengagement zone height is ~4-6 D. The fluidized bed is initialized with small, medium and large polymer particles.
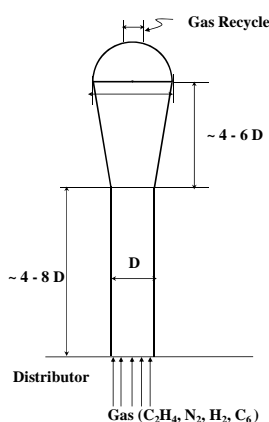
Figure 2: Sketch of pilot-plant fluidized-bed reactor.

The multi-fluid CFD model in FLUENT 6.3 is used to describe segregation of polymer particles due to hydrodynamic and electrostatic effects in gas-solid polymerization fluidized beds. Grid generation for the pilot-plant reactor geometry is done using the Gambit 2.3 software. A Cartesian coordinate system is used for grid generation and quadrilateral cells are formed for the two-dimensional case. Time-dependent simulations are performed for the pilot-plant reactor. Two-dimensional simulations are done as three-dimensional simulations are computationally expensive. **Table 1** shows the properties of solid and gas phases used in the pilot-plant simulations. The size and charge on each solid phase is normalized by the average values.

Solids (polymer)	Small	Medium	Large	Catalyst
density, kg/m^3	843.0	843.0	843.0	1000.0
d/d_{avg}	0.56	1.07	1.728	0.103
volume fraction	0.019	0.2316	0.25	0.0005*
q/q_{avg}	16.14	-4.776	-0.80	47.76**
Gas				
density, kg/m^3			22.1	
viscosity, kg/ms			1.427e-05	
velocity, m/s			0.61	

*continuously injected through the distributor plate
**the sign of charge is varied

Table 1: Properties of gas and solid phases used in the simulation.

Effect of catalyst overfeeding on the distribution of polymer particles

The objective of this simulation is to study the effect of a charge surge on the spatial distribution of polymer particles due to catalyst overfeeding. This would have obvious heat control problems due to the sudden increase in the reaction rate, but the effect this might have on the electrostatic forces in the bed has received scant attention. The idea is to observe whether more segregation is observed with an abnormally high degree of charge on the solid phases compared to the case with no charge. The mean bed charge is known to be negative from experimental results. The small polymer particles are positively charged, and the medium and large polymer particles are negatively charged. The three solid phases are uniformly distributed at the start of the simulation. Two cases are run with the above-stated simulation conditions. In the first case the charges on the solid phases are initialized to zero. In the second case there is a very high charge on each solid phase as shown in **Table 1**. It is important to emphasize that the high charge case is not typical of normal operation in a polymer fluid bed. However, abnormal upsets can occur during operation, and it is of interest to see the effect of these upsets as related to electrostatic events. The first case serves as a base case and is used to compare the results with the second case. The simulation parameters are shown in **Table 2**.

Description	Value
Pressure-based solver	2ddp (double precision)
Unsteady formulation	second-order implicit
Time step, sec	0.0001-0.0005
Data sampling for time statistics	1 time step
Momentum discretization	second-order methods
Boundary conditions	
Inlet	velocity inlet
outlet	pressure outlet
Wall	
gas phase	zero slip
solid phase	free slip
electric potential	zero

Table 2: Parameters used in the pilot-plant reactor simulations

The instantaneous contours of electric potential are shown in **Figure 3** for the case with particle charge. Due to hydrodynamic segregation, a higher volume fraction of the small positively charged polymer particles is observed in the expansion section. For this reason a positive potential is seen at the top of the reactor. Similarly higher volume fractions of the negatively charged medium and large polymer particles are observed in the fluidized zone. For this reason the electric potential is negative towards the bottom and near the distributor plate. In actual reactor operation there is evidence that shows that most electrostatic effects are found near the distributor plate and near the expansion and dome sections of the reactor.
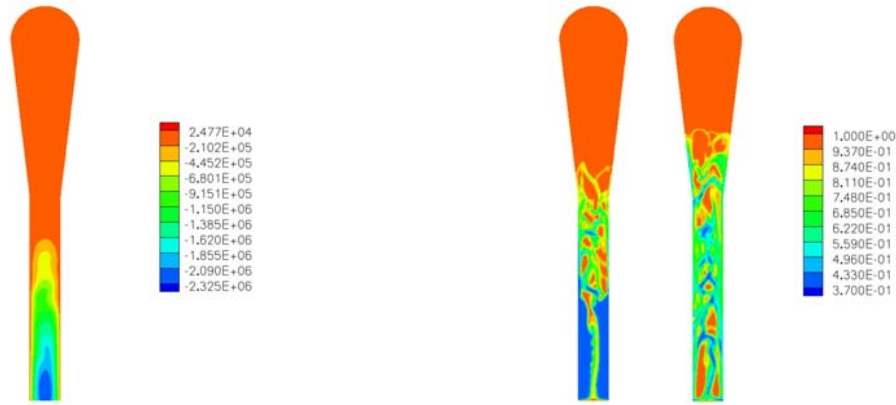
Figure 3: Instantaneous contours of electric potential (volts/m) with strongly charged particles.

Figure 4 shows the volume fractions of medium and large negatively charged polymer particles. From the basic electrostatic laws a negatively charged particle is pushed away from a region of high negative potential field and for this reason high volume fractions of negatively charged particles are seen close to the walls near the distributor plate. This condition can lead to defluidization. **Figure 5** shows the contours of volume fractions of gas for cases with and without catalyst overfeeding. With strong enough charge, the high volume fraction of medium and large particles (**Figure 4**) partially plugs the distributor plate and a non-uniform gas flow is observed. When there is no charge a more uniform gas flow is seen. The case of defluidization is observed when the polymer particles are highly charged. Another case is simulated with the magnitude of the charge on each solid phase is reduced by 60 percent. **Figure 6** shows the contours of volume fraction of the gas and solid phases with normal charges. A more uniform gas flow and lower volume fractions of medium and large polymer particles are observed than for the strongly charged case. Taken together these simulations indicate that the particle charge can lead to defluidization if sufficiently strong such as might occur due to catalyst feed upsets.

(a)   (b)
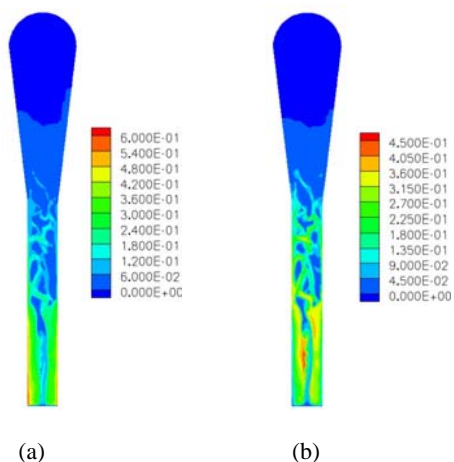
Figure 4: Instantaneous contours of solids volume fraction for (a) medium and (b) large particles with strong charges.

(a)   (b)

Figure 5: Instantaneous contours of volume fraction for the gas phase with (a) strongly charged particles and (b) particles without charge.

Continuous injection of catalyst particles

The objective of this simulation is to study the effect of the spatial distribution of injected catalyst particles. Catalyst is continuously injected into a bed of polymer particles using a catalyst feeder. The catalyst is injected into the side of the reactor about one reactor diameter above the plate. The mean bed charge is known to be negative and three cases are simulated where the polarity of the catalyst phase is varied. Low volume fractions of catalyst phase approximating realistic conditions are used. Three cases are run with different charges on the catalyst phase. A base case with zero, positive, and negative charge are considered.

(a)   (b)   (c)
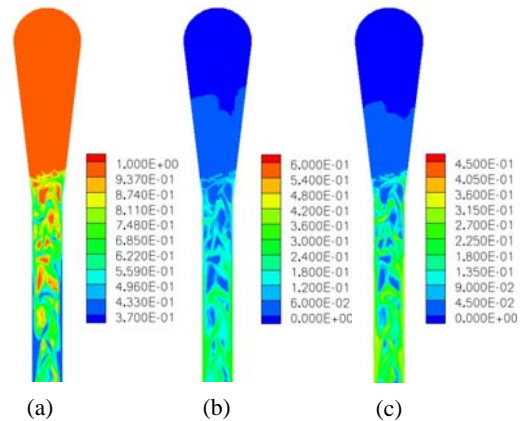
Figure 6: Instantaneous contours of volume fraction for (a) gas phase (b) medium particles, and (c) large particles with normal charges.

The instantaneous contour plot of volume fraction for the negatively charged catalyst phase is shown in **Figure 7.** Since the large particles are negatively charged and the mean bed charge is negative, the electric potential close to the injection point and near the distributor plate is negative. Thus, despite being subject to strong drag forces due to their small size, the negatively charged catalyst particles segregate to the lower sections of the walls of the reactor. This simulation is an example where the electrostatic effects are high compared to the drag forces.
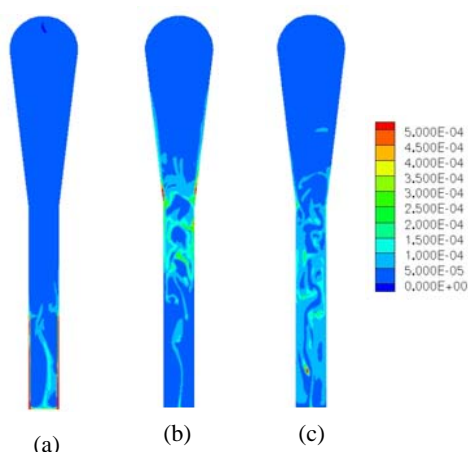
Figure 7: Instantaneous contours of catalyst with (a) negative charge, (b) positive charge and (c) zero charge.

In contrast to charged catalyst particles, uncharged catalyst particles followed the gas flow and are entrained out of the reactor. On the other hand, positively charged catalyst particles also follow the gas phase into the expansion section, but once there the positive electric potential pushes these particles towards the walls of the expansion and disengagement zones. High volume fractions of positively charged catalyst particles are present near the walls in the expansion section of the reactor, leading to a lower particle entrainment rate than observed for uncharged particles.

CONCLUSIONS

An electrostatic model was developed and coupled with a multi-fluid CFD model for gas-solid flows. These simulations show pronounced segregation due to electrostatic forces using sufficiently strong charges for gas-solid fluidized beds. This operation is representative of upset conditions such as might occur due to a catalyst feeder malfunction. Significant segregation of polymer particles is observed with strongly charged particles, and sufficiently high charges were shown to induce defluidization. The electric potential and electric field results predicted from simulations are in qualitative agreement with the available experimental observations in gas-solid fluidized beds. Simulations showed that the distribution of the catalyst phase depends on its charge and polarity relative to the polymer particles. However, by employing the known specific charges for different polymer particle sizes, the current model is able to give good qualitative estimates of the mean properties, such as the solid-phase spatial distribution and the pressure drop, and captures the trends observed when electrostatic effects are important. Current work focuses on applying the multi-fluid model with electrostatics forces to investigate full 3-D reactor configurations typical of plant-scale polymerization fluidized-bed reactors.

ACKNOWLEDGEMENTS

REFERENCES

BARON, T., BRIENS, C. L., BERGOUGNOU, M. A. AND HAZLETT, J.D., (1987), "Electrostatic effects on entrainment from a fluidized bed", Powder Tech. **53**, 55–67.

BRIENS, C. L., BERGOUGNOU, M. A., INCULET, I. I., BARON, T. AND HAZLETT, J. D. (1992), "Size distribution of particles entrained from fluidized beds: Electrostatic effects", Powder Tech. **70**, 57–62.

CROSS, J. A., (1987), "Electrostatics: Principles, Problems and Applications", Adam Hilger, Bristol.

FAN, R. AND FOX, R. O., (2008), "Segregation in polydispersed fluidized beds: Validation of a multi-fluid model", Chem. Eng. Sci. **63**, 272-285.

FAN, R., FOX, R. O. AND MUHLE, M. E., (2007), "Role of intrinsic kinetics and catalyst particle size distribution in CFD simulations of polymerization reactors", The 12th International Conference on Fluidization, Vancouver, Canada, May 13-17, 993-1000

FANG, W., JINGDAI, W. AND YONGRONG, Y., (2008), "Distribution of electrostatic potential in gas-solid fluidized bed and measurement of bed level", Ind. Eng. Chem. Res. **47**, 9517-9526.

GIDASPOW, D., (1994), "Multiphase Flow and Fluidization: Continuum and Kinetic Theory Descriptions". Boston. Academic Press.

HENDRICKSON, G., (2006), "Electrostatics and gas phase fluidized bed polymerization reactor wall sheeting", Chem. Eng. Sci. **61**, 1041-1064.

JACKSON, J. D., (1999), "Classical Electrodynamics", 3rd ed., New York: Wiley.

MAHDI, F. A., DUDLEY, A. S. AND SUNDARESAN, S., (2002), "The effect of static electrification on gas-solid flows in vertical risers", Ind. Eng. Chem. Res. **41**, 6224-6234.

MEHRANI, P., BI, H. T. AND GRACE, J. R., (2005), "Electrostatic charge generation in gas-solids fluidized beds", J. Electrost, **63**, 165-173.

MEHRANI, P., BI, H. T. AND GRACE, J. R., (2007), "Electrostatic behavior of different fines added to a Faraday cup fluidized bed", J. Electrost. **65,** 1-10.

SHIH, Y., GIDASPOW, D., AND WASAN, D., (1987), " Hydrodynamics of electro fluidization: Separation of pyrites from coal", AIChE J. 33, 1322-1333.

TORTORA, P. R., CECCIO, S. L. AND TORCZYNSKI, J. R., (2005), "The equivalent electrical permittivity of gas-solid mixtures at intermediate solid volume fractions", Sandia Report, Sandia National Laboratories.

VAN DER HOEF, M. A., VAN SINT ANNALAND, M., DEEN, N. D. AND KUIPERS, J. A. M., (2008), "Numerical simulation of dense gas-solid fluidized beds: A multiscale modeling strategy", Annu. Rev. Fluid Mech. **40**, 47–70.